11

Introduction to LED Backlight Driving Techniques for Liquid Crystal Display Panels

Huang-Jen Chiu[1], Yu-Kang Lo[1], Kai-Jun Pai[1], Shih-Jen Cheng[1],
Shann-Chyi Mou[2] and Shih-Tao Lai[3]
[1]*National Taiwan University of Science and Technology,*
[2]*Ching-Yun University,*
[3]*Chung-Yuan Christian University,*
Taiwan

1. Introduction

Liquid crystal display (LCD) is widely used in various display applications such as cellular phones, PC monitors, televisions (TVs), multimedia products, among others. An LCD backlight module usually includes backlight sources, a light-diffusion plate, a reflector, a brightness-enhancement film (BEF) and a light-guide plate (LGP). Conventionally, cold cathode fluorescent lamps (CCFLs) are required to provide sufficient backlighting for LCD panels [1-5]. Growing concerns about environmental issues will inhibit the use of CCFLs that contain poisonous mercury. Owing to improvement in long operative life, wider operation temperature range, and the simplicity of driver circuit work with low and safe voltages, light emitting diode (LED) has gradually substituted the CCFL as backlight [6-9]. This chapter will introduce some LED backlight driving techniques for LCD panels. Some dimming control methods will also be introduced and compared for regulating the LED current and brightness of the LED backlight system. The principal goal of this chapter is to ensure that readers become familiar with LED backlight driving techniques for LCD panels. We begin this chapter with a look at three LCD backlight structures: edge-light type, bottom-light type and hollow type. Figure 1(a) shows the bottom-light structure. Because of its high-luminance feature, the bottom-light structure is commonly used for PC monitors and TVs. With regard to the luminance uniformity on an LCD panel, a light-mixed zone is necessary between the diffusion plate and the light sources. This zone causes undesirable thickness for large-sized TV applications. Figure 1(b) shows the hollow type structure in which an LGP is used to reduce the thickness of the light-mixed zone. The good qualities of this type pertain to its compact shape, high luminance and good thermal dissipation. Figure 1(c) shows the edge-light structure commonly used in a small-scale LCD panel. This type is of compact shape and low power consumption, so it is suitable for notebook PCs and personal digital assistant (PDA) products. There are two types of LEDs for backlight sources, the white-light LEDs and RGB LEDs. The white-light LED is composed of a blue LED coated with yellow phosphor. Simple driving feature make it as a popular choice for new generation of LCD backlight sources in portable display products. Its color filter divides the emitted white light into RGB sub-pixels to present color pictures. Thicknesses of

Source: New Developments in Liquid Crystals, Book edited by: Georgiy V. Tkachenko,
ISBN 978-953-307-015-5, pp. 234, November 2009, I-Tech, Vienna, Austria

RGB sub-pixels must be adjusted according to the corresponding wavelengths to correct the white balance on LCD panel. This results in the difficulty of manufacturing process. The white-color point may vary after a long working time. Thus, the RGB LEDs mixing three-color lights to white light are more suitable for medium-scale, or even large-size screens [10-16]. White balance of the LCD panel with RGB LED backlight can be easily corrected by regulating the emission luminance of the RGB LEDs individually.

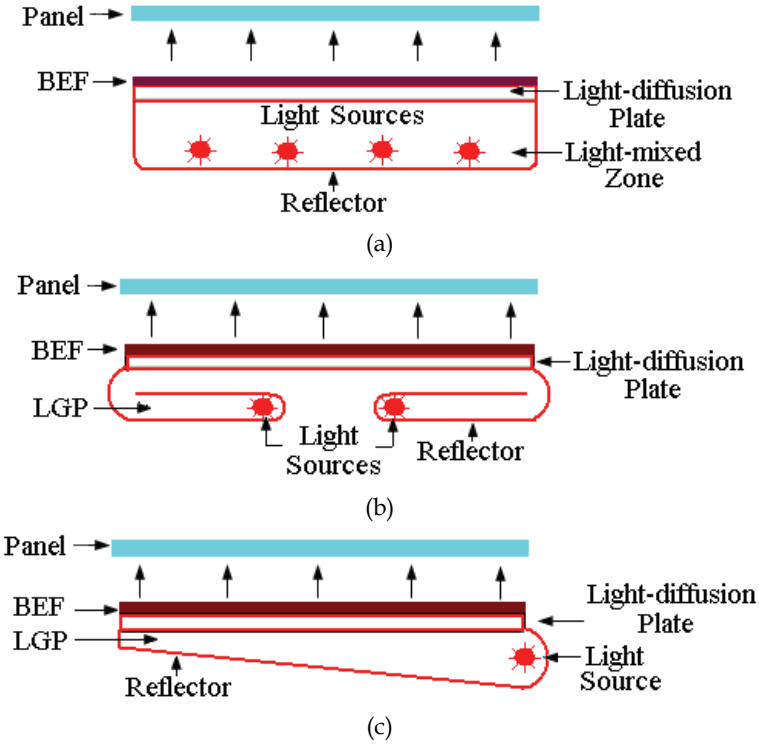

Fig. 1. (a) Bottom-light Type, (b) Hollow Type and (c) Edge-light Type Backlight Structures.

2. RGB LED backlight circuit

Figure 2 shows the block diagram of an LCD TV power supply with RGB LED backlight design. The LCD TV power provides a 12V output for the signal-process board, a 24V output for the backlight driving circuit and an additional 5V standby-power output. As shown in Figure 3, the backlight driving circuit consists of three power converters. Backlight LEDs are connected in series and parallel in the RGB LED backlight modules. LED current/voltage characteristic variations cause brightness difference. Therefore, dimming control is an important design consideration for LED backlight applications. We studied three dimming methods for current regulation of the parallel connected LED arrays: the transconductance-amplifier (TA) dimming, the current-mirror (CM) dimming and the burst-mode (BM) dimming.

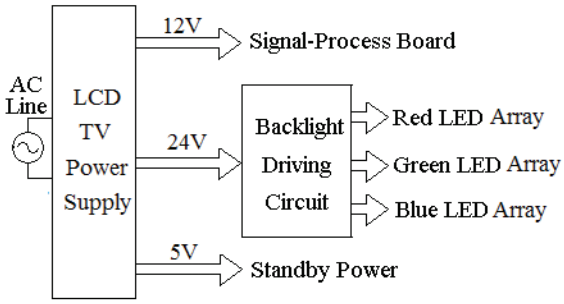

Fig. 2. Block Diagram of an LCD TV Power Supply.

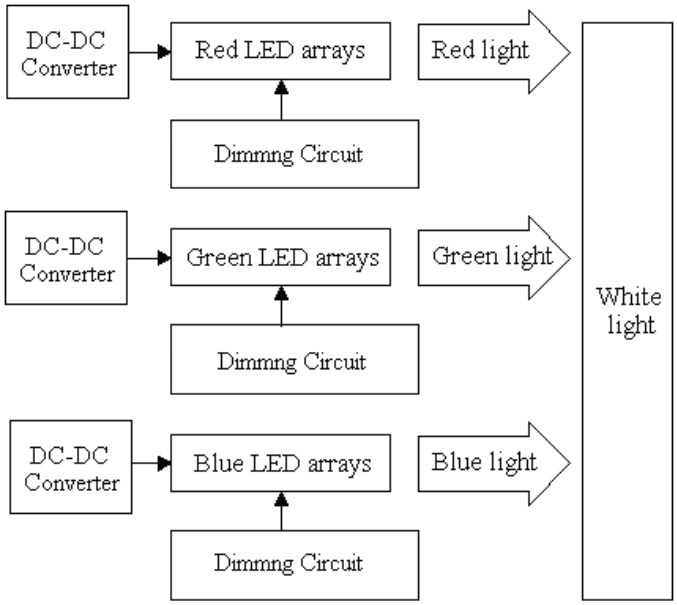

Fig. 3. RGB LED Backlight Driving Circuit

Figure 4(a) shows the TA dimming circuit. The LED current can be expressed as Equation (1).

$$I_{LED} = \frac{V_d}{R}, \tag{1}$$

Figure 4(b) shows the CM dimming circuit. The LED current can be expressed as Equation (2).

$$I_{LED} \approx I_r = K_n (V_{GS} - V_{TN})^2 = \frac{V_d - V_{GS}}{R}, \tag{2}$$

where K_n and V_{TN} are the conduction parameter and threshold voltage of the dimming transistors Q_r and Q_d, respectively. By using the TA dimming and CM dimming circuits, the

current regulation of paralleled LED arrays can be achieved. However, the conduction losses of the dimming transistors will be difficult to solve [17]. An adaptive voltage output for the DC-DC converter is usually designed to retain the minimum drain-source voltage on the dimming transistors. As shown in Figure 4(c), the backlight LED current can be also controlled with a BM dimming circuit. Considering the switching loss for the dimming transistors, the burst-mode frequency f_b is designed at 400Hz that are unperceivable to the human eye. The duty ratios of the dimming transistors are varied to regulate the LED average current that can be represented as Equation (3).

$$I_{LED(av)} = I_m \delta, \tag{3}$$

where I_m denotes the peak value of the LED array current. The dimming transistors are operated as low-frequency switches, the thermal problem on the dimming transistors can be improved significantly. The current variations can be minimized by using the TA or BM dimming methods while the CM dimming has the simplest circuit configuration. Anyway, the TA and CM dimming methods are unsuitable to be used in the high-power LED backlight design of LCD panels due to the significant conduction losses of the dimming transistors under dimming operations. The emission luminance of the RGB LEDs is able to be regulated individually for achieving the white balance of the LCD panel. The luminance of the red light is always highest and the luminance of the blue light is lowest among three color lights. In practical applications, the blue light is most sensitive to human eyes such that lower luminance of blue LED is enough to compose white light with the red and green LEDs.

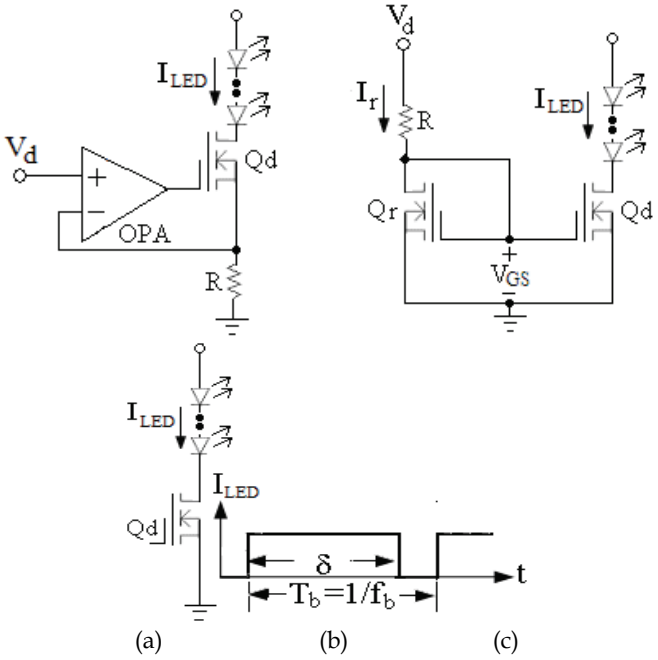

Fig. 4. (a) TA, (b) CM and (c) BM Dimming Methods

3. Soft-switched LED backlight circuit

Figure 5(a) shows a half-bridge DC-DC Series-Resonant Converter (SRC) topology for driving the RGB LEDs. The soft-switched DC-DC resonant converter includes power switches Q_1 and Q_2, resonant inductor L_r, resonant capacitor C_r, transformer T_1, rectifier diodes D_{f1} and D_{f2}, filter capacitor C_f, and the LED arrays represented by an equivalent resistance R_o. The characteristic impedance and the resonant frequency are respectively [18-21].

$$Z_c = \sqrt{\frac{L_r}{C_r}}, \tag{4}$$

$$f_r = \frac{1}{2\times\pi\times\sqrt{L_r C_r}}, \tag{5}$$

From (4) and (5), L_r and C_r can be expressed as

$$\mathrm{L_r} = \frac{\mathrm{Z_c}}{2\times\pi\times\mathrm{f_r}}, \tag{6}$$

$$\mathrm{C_r} = \frac{1}{2\times\pi\times\mathrm{f_r}\times\mathrm{Z_c}}, \tag{7}$$

The turn number of the primary winding is

$$\mathrm{N_p} = \frac{(\mathrm{V_{Np}} - 1)\times 10^8}{4\times\mathrm{f_s}\times\mathrm{B_r}\times\mathrm{A_e}}, \tag{8}$$

where V_{Np} is the peak-to-peak amplitude of the transformer primary voltage v_{Np}, f_s is the switching frequency, B_r is the magnetic flux density, and A_e is the effective core area. To simplify the analysis, the first-order harmonic approximation has been applied, and the circuit elements of the primary side in Figure 5(a) are reflected to the secondary side, as depicted in Figure 5(b). The equivalent impedances Z_1 and Z_2 are respectively

$$\mathrm{Z_1} = \frac{\mathrm{n^2}}{\mathrm{j\omega C_r}} + \mathrm{j\omega n^2 L_r}, \tag{9}$$

$$Z_2 = j\omega n^2 L_m // R_o, \tag{10}$$

where $n=N_s/N_p$.
The voltage divider rule can be used to obtain the output voltage phasor V_L as

$$V_L = V_{in}\left(\frac{Z_1}{Z_1 + Z_2}\right), \tag{11}$$

where the amplitude of V_L is assumed equal to V_o. V_{in} is the phasor of the fundamental component of v_a in Figure 5(a).

$$\left|V_{in}\right| = \frac{n}{\pi} V_s, \tag{12}$$

Substituting (9), (10) and (12) into (11), the voltage gain transfer function can be expressed as

$$\left|\frac{V_o}{V_s}\right| = \frac{n\omega^2 L_m C_r R_o}{\pi\sqrt{[R_o - \omega^2 C_r R_o (L_r + L_m)]^2 + [n^2 \omega L_m (1 - \omega^2 L_r C_r)]^2}}, \tag{13}$$

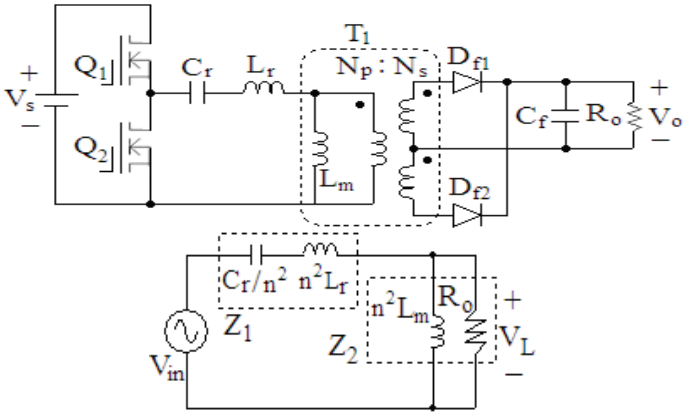

(a) (b)

Fig. 5. (a) Half-bridge DC-DC SRC Topology and (b) Its Equivalent Circuit.

It is clearly seen from (13) that the switching frequency must be varied to regulate the output voltage. The highest switching frequency appears at the highest input voltage and the lightest load. On the other hand, the lowest switching frequency happens at the lowest input voltage and the heaviest load. For the SRC to operate in the zero-voltage-switching (ZVS) region, the lowest switching frequency must be higher than the resonant frequency as expressed in (5). Moreover, due to the switching speed limitations of the power devices, the highest switching frequency is below a specified value. In other words, the variations of the input DC voltage and the load variations must be confined to a small range. Usually a power factor corrector (PFC) is added in front of the DC-DC converter to raise the input power factor and reduce the input current harmonics. A phase-shift pulse width modulation (PSPWM) dimming control can effectively confine the load variation of the DC-DC SRC. Consequently, the output voltage variation of the PFC can be limited to a smaller extent. This results in a better operating condition for the SRC. For the PSPWM dimming strategy, the working durations of the shunt LED arrays are properly phase-shifted to confine the variation of the output current of the SRC. Figure 6 illustrates the circuit arrangement for N shunt single-colored LED arrays with PSPWM dimming method. It is almost the same as the conventional one, except that the dimming signals are applied with a specified phase difference. With the PSPWM dimming, there are always overlaps between the LED driving currents. The maximum duty cycle, or the overlap, is 100 %, corresponding to the highest brightness. To prevent the DC-DC SRC from operating at no load, the minimum duty cycle of the PSPWM dimming signal is 1/N, where N is the number of the shunt LED arrays.

Under this circumstance, the overlap is zero, corresponding to the lowest brightness. Compared with the conventional dimming scheme, it is apparently recognized that the load variation of the SRC is less with the proposed PSPWM dimming function. To further investigate the operating principle of the PSPWM dimming, a more general case with N shunt LED arrays is discussed as follows. Figure 7 shows the waveforms of the N driving currents and the output current of the SRC. As stated earlier, the duty cycle range of the dimming signal is from 1/N to 100 %. In terms of the phase angle, if a complete period is 360°, the duty cycle range is from 360°/N to 360°. Assuming that the dimming signal for the LED array 1 starts at 0°, then the dimming signal for the k-th LED array would start at

$$\phi_k = 360^o \times (k-1)/N, \tag{14}$$

If the duty cycle of each dimming signal is ϕ_d, then the average driving current of one LED array is

$$I_{avg} = \phi_d \times I_p / 360^o, \tag{15}$$

where I_p is the amplitude of the driving current for each LED array. Therefore the average output current of the SRC is

$$I_{o,avg} = \phi_d \times I_p \times N / 360^o, \tag{16}$$

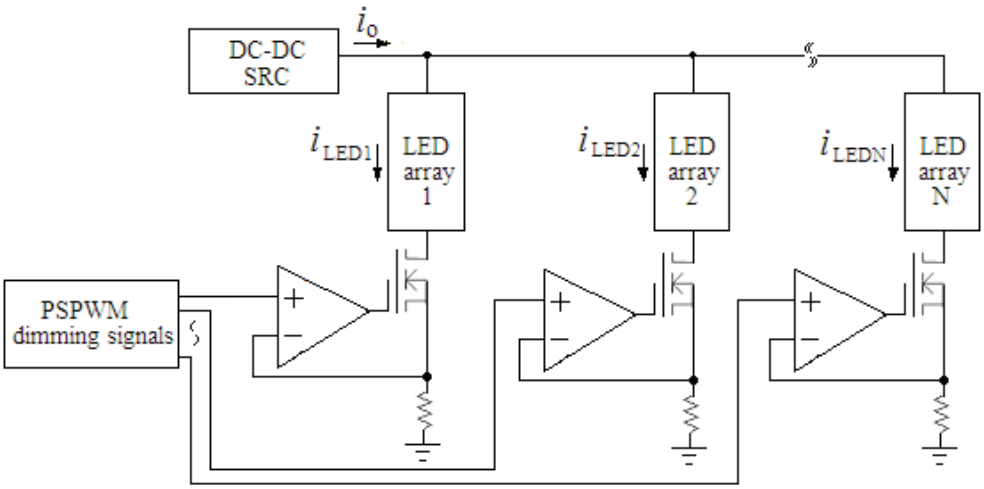

Fig. 6. The PSPWM Dimming Method.

It can be observed from Figure 7 that if the end of the dimming signal for LED array 1 is at ϕ_d, where ϕ_d is between ϕ_k and ϕ_{k+1} and $k \neq 1$, then the output current of the SRC in the range of ϕ_k to ϕ_{k+1} is

$$i_o = \begin{cases} kI_p & for\ \phi_k \le \phi \le \phi_d \\ (k-1)I_p & for\ \phi_d \le \phi \le \phi_{k+1} \end{cases}, \tag{17}$$

This is also the SRCs output current in each duration from ϕ_j to ϕ_{j+1}, where j = 1 to N. Therefore, the average output current of the SRC is now

$$I_{o,avg} = \frac{kI_p \times [\phi_d - 360^o / N \times (k-1)] + (k-1)I_p \times [360^o / N \times k - \phi_d]}{360^o / N}, \quad (18)$$
$$= N \times \phi_d \times I_p / 360^o$$

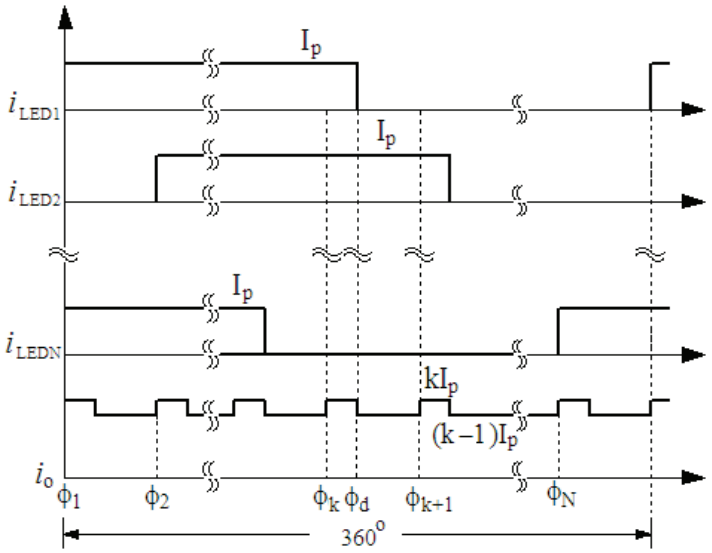

Fig. 7. Current Waveforms of N Shunt LED Arrays for the PSPWM dimming.

A favored feature is that the load variation of the SRC is always within one step change of I_p, no matter what the load level is. Therefore, by carefully designing the duty cycle and the amplitude of the driving current for each LED array, the no load operation of the DC-DC SRC may be precluded. Moreover, the output transient of the SRC is improved due to the confined load change. The number of the LED array for one color, and the peak driving current of each LED array are first determined according to the specifications of the LED and the spectrum of the white color. Then a suitable duty cycle is chosen allowing a reasonable span of variation for dimming control.

4. Single-stage LED backlight circuit

Figure 8 shows a single-stage LED backlight driving system. The backlight driving system consists of an AHB DC/DC cell integrated with a charge-pump PFC cell. The power MOSFETs Q1 and Q2, operate with asymmetrical duty ratios, δ and 1-δ, which require short and well-defined dead time between the conduction intervals. D1, D2 and C_{p1} and C_{p2} are the body diodes and the parasitic capacitors of power MOSFETs, respectively. The charge-pump PFC cell is composed of resonant inductor L_r, charge-pump capacitors C_{r1} and C_{r2}, input diodes D_{i1}, and D_{i2}, clamping diodes D_{c1}, and D_{c2}. The capacitor C_{bus} is used as the DC bus capacitor between the charge-pump PFC cell and the post-stage AHB DC/DC cell. The

transformer leakage inductor L_l resonates with the parasitic capacitors C_{p1} and C_{p2} during dead-time intervals to achieve zero-voltage switching for the power MOSFETs. The blocking capacitor C_b is used to assure that the power sent into the transformer primary winding is a pure AC type. A DC voltage is supplied to the LED arrays through the secondary rectifier and filter circuit that are composed of D3, D4, L_o and C_o.

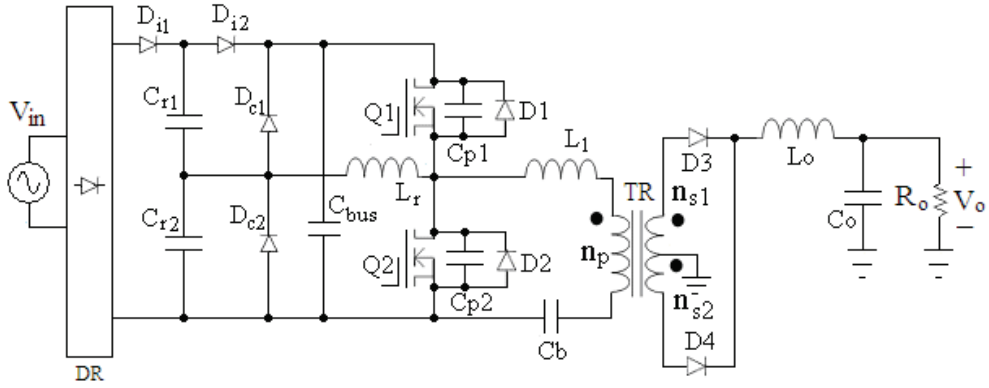

Fig. 8. Single-stage LED Backlight Driving System.

The average rectified input current $|I_{in}|_{,av}$ can be expressed as follows.

$$|I_{in}|_{,av} = \frac{\Delta Q}{T_s} = f_s C_{r1} |V_{in}|, \tag{19}$$

where ΔQ is the charge variation of C_{r1}. From Equation (19), we can see that the average rectified input current is proportional to the rectified input voltage. Thus, high power factor can be achieved. Based on the power balance between the input and output of the AC/DC converter, the following equation has to be satisfied.

$$|I_{in}|_{,av} = \frac{2P_o}{\eta V_{in}^{\,2}} |V_{in}|, \tag{20}$$

where η and Po are the overall efficiency and output power of the converter. From Equations (19) and (20), the design equations for the resonant inductor L_r and the charge-pump capacitor C_{r1} can be derived as follows [22-25].

$$L_r = \frac{\eta V_{in}^{\,2}}{8\pi^2 f_s P_o}, \tag{21}$$

$$C_{r1} = \frac{2P_o}{\eta f_s V_{in}^{\,2}}, \tag{22}$$

The ZVS conditions for power switches depend on the resonant inductance current I_{Lr} related with the input voltage. At the zero-crossing of input voltage, the resonant inductance current I_{Lr} will be ignorable. Considering the ZVS condition during an entire a

line period, the transformer leakage inductance L_l could be determined by using Equation (23).

$$L_l \geq (C_{p1} + C_{p2})[\frac{n_p V_{bus}}{min(n_{s1}, n_{s2})I_o}]^2, \quad (23)$$

In practical design, an external inductor L_e is usually needed to be added in series connected with L_l for satisfying ZVS condition [26-28]. The input current has a near sinusoidal waveform and in phase with the input voltage. High efficiency and high power factor can be achieved because of single-stage power conversion with soft-switching features.

5. Conclusion

The advantages of LED backlighting over conventional CCFLs are numerous: fast response, broader color spectrum, longer life span, and no mercury. However, CCFLs still have cost advantages. For a LED backlighting, luminous efficacy and thermal management are the most important issues need to be solved before commercialization. Anyway, rapid advances in material and manufacturing technologies will enable significant developments in high-luminance LEDs for backlighting applications. In this chapter, we introduced some LED backlight driving systems for LCD panels. Dimming control methods are then discussed to regulate the LED current and brightness for the LED backlight system.

6. References

[1] C. H. Lin, "The Design and Implementation of a New Digital Dimming Controller for the Backlight Resonant Inverter," *IEEE Trans. Power Electronics*, vol. 20, no. 6, pp. 1459-1466, Nov. 2005.

[2] C. G. Kim, K. C. Lee, and B. H. Cho, "Modeling of CCFL using Lamp Delay and Stability Analysis of Backlight Inverter for Large Size LCD TV," *IEEE APEC'05*, Vol. 3, pp. 1751-1757.

[3] Y. H. Liu, "Design and Implementation of an FPGA-Based CCFL Driving System With Digital Dimming Capability," *IEEE Transactions on Industrial Electronics*, Vol. 54, Issue 6, pp. 3307-3316, Dec. 2007.

[4] C. H. Lin, "Digital-Dimming Controller with Current Spikes Elimination Technique for LCD Backlight Electronic Ballast," *IEEE Transactions on Industrial Electronics,* Vol. 53, Issue 6, pp. 1881-1888, Dec. 2006.

[5] Y. K. Lo, and K. J. Pai, "Feedback Design of a Piezoelectric Transformer-based Half-bridge Resonant CCFL Inverter," *IEEE Trans. Industrial Electronics*, vol. 54, no. 4, pp. 2716-2723, Oct. 2007.

[6] K. H. Lee, and S. W. R. Lee, "Process Development for Yellow Phosphor Coating on Blue Light Emitting Diodes (LEDs) for White Light Illumination," *in Proc. Electronics Packaging Technology Conference*, 2006, pp. 379-384.

[7] T. Taguchi, Y. Uchida, and K. Kobashi, "Efficient White LED Lighting and Its Application to Medical Fields," *Journal of physica status solidi (a)*, vol. 201, no. 12, pp. 2730-2735, Sept. 2004.

[8] N. Mohan, T. M. Undeland, and W. P. Robbins, "Power Electronics," USA: John Wiley & Sons, 2003, pp. 301-313.

[9] H. van der Broeck, G. Sauerlander, and M. Wendt, "Power Driver Topologies and Control Schemes for LEDs," *in IEEE Proc. APEC'07*, 2007, pp. 1319-1325.

[10] C. C. Chen, C. Y. Wu, Y. M. Chen, and T. F. Wu, "Sequential Color LED Backlight Driving System for LCD Panels," *IEEE Transactions on Power Electronics*, Vol. 22, Issue 3, pp. 919-925, May 2007

[11] H. J. Chiu and S. J. Cheng; "LED Backlight Driving System for Large-Scale LCD Panels," I*EEE Transactions on Industrial Electronics*, Vol. 54, Issue 5, pp.:2751-2760, Oct. 2007.

[12] G. Park; T. S. Aum, J. H. Bae, J. H. Kwon, S. K. Lee; M. H. Lee and H. S. Soh, "Optimization of Direct-type LCD Backlight Unit," *Pacific Rim Conference on Lasers and Electro-Optics*, Aug. 2005, pp. 205-206.

[13] S. Y. Lee, J. W. Kwon, H. S. Kim, M. S. Choi and. S. Byun, "New Design and Application of High Efficiency LED Driving System for RGB-LED Backlight in LCD Display;" *the 37th IEEE Power Electronics Specialists Conference*, June 2006, pp.1-5.

[14] S. Muthu, F. J. Schuurmans, and M. D. Pashley, "Red, Green, and Blue LED based White Light Generation: Issues and Control," *Annual Meeting. Conference Record of the Industry Applications Conference*, Oct. 2002, Vol. 1, pp. 327-333.

[15] F. Bernitz, O. Schallmoser, and W. Sowa, "Advanced Electronic Driver for Power LEDs with Integrated Colour Management," *Annual Meeting. Conference Record of the Industry Applications Conference*, Vol. 5, Oct. 2006, pp. 2604-2607.

[16] C. C. Chen, C. Y. Wu, and T. F. Wu, "Fast Transition Current-Type Burst-Mode Dimming Control for the LED Back-Light Driving System of LCD TV," *IEEE Power Electronics Specialists Conference*, June 2006, pp. 1-7.

[17] Donald A. Neamen, "Electronic Circuit Analysis and Design, 2e," McGraw-Hill, 2001.

[18] C. C. Chen, C. Y. Wu, and T. F. Wu, "LED Back-light Driving System for LCD Panels," *IEEE APEC '06*, pp. 381-385.

[19] S. Y. Lee, J. W. Kwon, H. S. Kim, M. S. Choi, and K. S. Byun, "New Design and Application of High Efficiency LED Driving System for RGB-LED Backlight in LCD Display, " *IEEE PESC '06*, pp.1-5.

[20] M. Rico-Secades, A. J. Calleja, J. Ribas, E. L. Corominas, J. M. Alonso, J. Cardesin, and J. Garcia-Garcia, "Evaluation of a Low-Cost Permanent Emergency Lighting System based on High-Efficiency LEDs," *IEEE Transactions on Industry Applications*, Vol. 41, No. 5, Sept.-Oct. 2005, pp.1386-1390.

[21] H. Sugiura, S. Kagawa, H. Kaneko, M. Ozawa, H. Tanizoe, T. Kimura, and H. Ueno, "Wide Color Gamut Displays using LED Backlight- Signal Processing Circuits, Color Calibration System and Multi-Primaries," *IEEE ICIP'05*, Vol. 2, pp. 9-12.

[22] G. Moschopoulos and P. Jain, "Single-Phase Single-Stage Power-Factor-Corrected Converter Topologies," *IEEE Transactions on Industrial Electronics*, Vol. 52, Issue 1, pp.23–35, Feb. 2005.

[23] F. S. Kang, S. J. Park, and C. U. Kim, "ZVZCS Single-Stage PFC AC-to-DC Half-Bridge Converter," *IEEE Transactions on Industrial Electronics*, Vol. 49, Issue 1, pp.206-216, Feb. 2002.

[24] J. Qian, and F. C. Y. Lee, "A High-Efficiency Single-Stage Single-Switch High-Power-Factor AC/DC Converter with Universal Input," *IEEE Transactions on Power Electronics*, Vol. 13, No. 4, July 1998, pp.699-705.

[25] J. Qian, and F. C. Lee, "Charge Pump Power-Factor-Correction Technologies. II. Ballast Applications," *IEEE Transactions on Power Electronics*, Vol. 15, No.1, pp. 130-139, Jan. 2000.

[26] F. Bernitz, O. Schallmoser, and W. Sowa, "Advanced Electronic Driver for Power LEDs with Integrated Colour Management," *IEEE IAS'06*, Vol. 5, pp. 2604-2607.

[27] S. Muthu and J. Gaines, "Red, Green and Blue LED-based White Light Source: Implementation Challenges and Control Design," *IEEE IAS'03*, Vol. 1, pp. 515-522.

[28] S. Muthu, F. J. Schuurmans, and M. D. Pashley, "Red, Green, and Blue LED based White Light Generation: Issues and Control," *IEEE IAS'02*, Vol. 1, pp. 327-333.

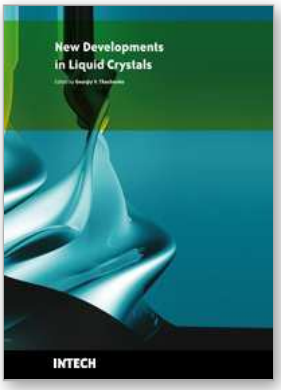

New Developments in Liquid Crystals

Edited by Georgiy V Tkachenko

ISBN 978-953-307-015-5
Hard cover, 234 pages
Publisher InTech
Published online 01, November, 2009
Published in print edition November, 2009

Liquid crystal technology is a subject of many advanced areas of science and engineering. It is commonly associated with liquid crystal displays applied in calculators, watches, mobile phones, digital cameras, monitors etc. But nowadays liquid crystals find more and more use in photonics, telecommunications, medicine and other fields. The goal of this book is to show the increasing importance of liquid crystals in industrial and scientific applications and inspire future research and engineering ideas in students, young researchers and practitioners.

How to reference

In order to correctly reference this scholarly work, feel free to copy and paste the following:

Huang-Jen Chiu, Yu-Kang Lo, Kai-Jun Pai, Shih-Jen Cheng, Shann-Chyi Mou and Shih-Tao Lai (2009). Introduction to LED Backlight Driving Techniques for Liquid Crystal Display Panels, New Developments in Liquid Crystals, Georgiy V Tkachenko (Ed.), ISBN: 978-953-307-015-5, InTech, Available from: http://www.intechopen.com/books/new-developments-in-liquid-crystals/introduction-to-led-backlight-driving-techniques-for-liquid-crystal-display-panels

INTECH
open science | open minds

InTech Europe
University Campus STeP Ri
Slavka Krautzeka 83/A
51000 Rijeka, Croatia
Phone: +385 (51) 770 447
Fax: +385 (51) 686 166
www.intechopen.com

InTech China
Unit 405, Office Block, Hotel Equatorial Shanghai
No.65, Yan An Road (West), Shanghai, 200040, China
中国上海市延安西路65号上海国际贵都大饭店办公楼405单元
Phone: +86-21-62489820
Fax: +86-21-62489821